

Supplement

Jize Jiang^{1,a,b}, David S. Stevenson¹, Aimable Uwizeye², Giuseppe Tempio², Alessandra Falcucci², Flavia Casu², and Mark A. Sutton³

¹School of GeoSciences, The University of Edinburgh, Crew Building, Alexander Crum Brown Road, Edinburgh, EH9 3FF, UK

²Food and Agriculture Organization of the United Nations, Animal Production and Health Division, Viale delle Terme di Caracalla, 00153 Rome, Italy

³UK Centre for Ecology and Hydrology, Edinburgh, Bush Estate, Midlothian, Penicuik, EH26 0QB, UK

^anow at: Institute of Agricultural Sciences/Institute of Biogeochemistry and Pollutant Dynamics, ETH Zurich, 8092 Zurich, Switzerland

^bnow at: Eawag, Swiss Federal Institute of Aquatic Science and Technology, Ueberlandstrasse 133, 8600 Dübendorf, Switzerland

Correspondence to: Jize Jiang (jize.jiang@usys.ethz.ch)

S1 Two-film model for the gas exchange across the air-liquid interface

The two-film model proposed by Liss and Slater (1974) for estimating the gaseous flux across the air-liquid interface is used to model the NH₃ emissions from pit storage in animal houses and lagoon systems in the AMCLIM model because these systems hold large amount of water (as mentioned in Sect.2.2.3 and 2.3.2). In this model, exchange is simulated to take place between two surface films, in the aqueous phase and gas phase respectively, as compared with the surrounding waterbody and air. Figure S1 illustrates the flux of NH₃ transferred from the liquid to the air across the interface. The main body of the liquid is assumed to be well-mixed, so the main resistances are from the gas and liquid phase interfacial layers (gas and liquid “films”). There are two transport processes. The first process is TAN from the bulk liquid to the interface ($F_{\text{TAN to surface}}$) through molecular transfer that is driven by concentration gradients, which can be expressed as:

$$F_{\text{TAN to surface}} = k_L([\text{TAN (aq)}]_{\text{bulk liquid}} - [\text{TAN (aq)}]_{\text{interface}}), \quad (\text{S1})$$

where k_L (m s⁻¹) is an aqueous transfer coefficient for TAN (NH₃ and NH₄⁺). The second process is NH₃ transported from the interface to the atmosphere (house atmosphere for housing simulations and free atmosphere for lagoon simulations), which can be expressed as:

$$F_{\text{NH}_3} = k_G([\text{NH}_3(\text{g})]_{\text{interface}} - [\text{NH}_3(\text{g})]_{\text{in/atm}}), \quad (\text{S2})$$

where k_G (m s⁻¹) is a gaseous transfer coefficient for NH₃. The aqueous TAN concentration and the gaseous NH₃ concentration at the interface is in equilibrium, and it is assumed that the transfer of NH₃ across the interface is in a steady state so that the two transport processes in aqueous and gaseous phase are equivalent.

$$k_L([\text{TAN (aq)}]_{\text{bulk liquid}} - [\text{TAN (aq)}]_{\text{interface}}) = k_G([\text{NH}_3(\text{g})]_{\text{interface}} - [\text{NH}_3(\text{g})]_{\text{in/atm}}). \quad (\text{S3})$$

In AMCLIM, the calculations of NH₃ emissions and other transport processes, such as diffusion, use resistances, some of which are the reciprocals of the transfer coefficients as shown in Eq. (3). In addition, as NH₃ emissions take place from wet

surfaces, the gaseous NH₃ concentration at the interface in the two-film model is represented by χ_{srf} in AMCLIM. By combining Eqs. S1-S3, the NH₃ emission can be calculated by simulating the TAN concentration of the bulk liquid using the following equation (under the simplification that atmospheric indoor NH₃ concentrations are 0; as expressed by Eq. S4):

$$F_{\text{NH}_3} = \frac{\chi_{\text{srf}}}{R_G} = \frac{[\text{TAN (aq)}]}{R_{GL}}, \quad (\text{S4})$$

where R_{GL} is a combined resistance that limits the NH₃ transfer across the gas-liquid interface, which is expressed as:

$$R_{GL} = \frac{1}{k_L} + \frac{1}{k_G K_{\text{NH}_3}}. \quad (\text{S5})$$

The aqueous and gaseous transfer coefficients are empirically derived (Ni, 1999), which are calculated by the following equations:

$$k_L = 1.417 \times 10^{-12} T^4, \quad (\text{S6})$$

$$k_G = 0.001 + 0.0462 u_* Sc^{0.67}, \quad (\text{S7})$$

where Sc is the Schmidt number which is calculated from the kinematic viscosity (ν , m² s⁻¹) and diffusivity of NH₃ as

follows:

$$Sc = \frac{\nu}{D_{\text{NH}_3}^{\text{gas}}}, \quad (\text{S8})$$

$$\nu = 1.56 \times 10^{-5} \left(\frac{T+273.15}{298.15} \right)^{\frac{3}{2}}. \quad (\text{S9})$$

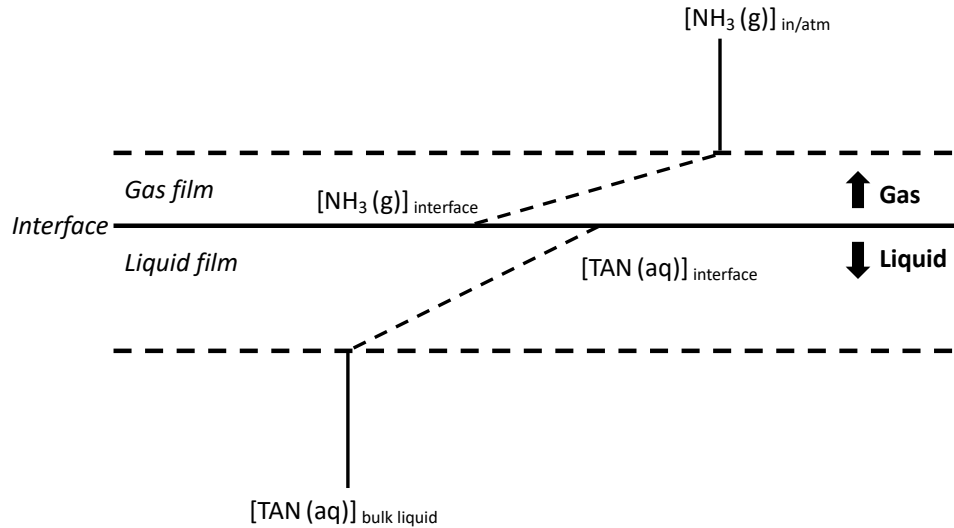


Figure S1. Sketch of the ammonia transfer processes across an air-liquid interface ('two-film model' adapted from Liss and Slater, 1974). In AMCLIM, $[\text{NH}_3(\text{g})]_{\text{interface}}$ in the figure is represented by χ_{srf} , and $[\text{NH}_3(\text{g})]_{\text{in/atm}}$ is represented by χ_{in} or χ_{atm} .

S2 Hydrolysis of urea/uric acid and mineralization of organic nitrogen

The conversion rates of multiple nitrogen forms (e.g., urea, UA and other organic nitrogen) to TAN is specified by the term K (s^{-1}). The rate of conversion is dependent on environmental factors, such as temperature, RH, water content and the pH of soils or manure. The hydrolysis rate of urea (K_{Urea} , s^{-1}) is parameterized as follows by assuming a first order reaction according to (Sherlock and Goh, 1984):

$$\frac{dM_{Urea}}{dt} = -K_{Urea}M_{Urea}, \quad (S10)$$

$$K_{Urea} = 1 - \exp(-k_h \cdot WFPS \cdot A_h), \quad (S11)$$

$$A_h = 0.25 \exp(0.0693(T - 273.15)), \quad (S12)$$

where k_h is the urea hydrolysis constant for urine ($6.4 \times 10^{-5} s^{-1}$ or $0.23 h^{-1}$; Sherlock and Goh, (1984)) and for urea in soils ($8.3 \times 10^{-6} s^{-1}$ or $0.03 h^{-1}$; Dutta et al. (2016)). Real urine from animals is found to have a faster decomposition rate than chemical urea fertilizer (Haynes and Williams, 1993; Sherlock and Goh, 1985). $WFPS$ is the water-filled pore space and is set to 1 for livestock urine. A_h is a temperature correction dependence, and T is the temperature in Kelvin (K).

The hydrolysis rate of uric acid (K_{UA} , s^{-1}) is calculated from the product of a series of conversion rate functions (Elliott and Collins, 1982), as follows:

$$K_{UA} = 0.2k_{pH}k_Tk_{RH}, \quad (S13)$$

where k_{pH} , k_T and k_{RH} are the functions of pH, temperature and RH influencing uric acid hydrolysis rate, respectively. The maximum estimated hydrolysis rate of uric acid is $0.2 d^{-1}$. The temperature (in $^{\circ}C$), RH and pH dependence of UA hydrolysis rate is shown by the following equations:

$$k_T = \frac{\exp(0.149(T-273.15)+0.49)}{\exp(0.149(35)+0.49)} \quad (S14)$$

The temperature dependence follows an exponential relationship and is normalised to the maximum rate at $35^{\circ}C$ (Jiang et al., 2021). The relative humidity dependence is specified as:

$$k_{RH} = 0.0124 RH - 0.0014 \quad (S15)$$

The RH dependence increases linearly as RH increases, reaching the maximum rate of 1 at RH 80 % (Jiang et al., 2021). Note that the humidity level can be a key limiting factor in determining the rate of uric acid hydrolysis and subsequent TAN emissions. The pH dependence is specified as:

$$k_{pH} = \frac{1.34(pH)-7.2}{1.34(9)-7.2} \quad (S16)$$

A fixed pH of 8.5 is applied as the typical value of poultry manure (Elliott and Collins, 1982; Sommer and Hutchings, 2001), see Table A1.

Organic N (other than urea and uric acid) is categorised into three types: a) available organic nitrogen, b) resistant organic nitrogen and c) unavailable organic nitrogen, referring to how readily that the organic nitrogen is available to decompose to form TAN (Riddick et al., 2016). A fraction of 50 % organic nitrogen is assumed to be available organic nitrogen, 45 % is in

the resistant form, and the rest of 5 % goes to the unavailable nitrogen pool (Riddick et al., 2016). The rate of mineralization of organic nitrogen is determined by the following equation:

$$85 \quad K_{\text{ORG N}} = B_{a,r} A_m, \quad (\text{S17})$$

$$A_m = t_{r1} \exp(t_{r2}(T - 273.15)), \quad (\text{S18})$$

where $B_{a,r}$ ($B_a = 8.94 \times 10^{-7} \text{ s}^{-1}$; $B_r = 6.38 \times 10^{-8} \text{ s}^{-1}$) are the mineralization constants for available and resistant organic N (Gilmour et al., 2003; Vigil and Kissel, 1995). A_m is a temperature correction dependence, with t_{r1} and t_{r2} are equivalent to 0.0106 K^{-1} and 0.12979 K^{-1} , respectively.

90 **S3 Housing simulations for pigs, poultry and ruminants**

S3.1 Simulations for pig housing

AMCLIM–Housing includes three types of animal houses, as introduced in Section 2.2.1: pig houses with slatted floors, pig barns and deep litter poultry houses. The first housing type has slatted floor and pit storage has been described in Sect 2.2.3.

95 The second house type is a normal barn with a solid floor (without pit storage). In AMCLIM–Housing, normal barns are assumed to be cleaned daily so that pig excreta are removed from the house, and all pools are reset to zero every day. Volatilization of NH_3 from the pig excreta on the solid floor is identical to the processes taking place on the slats in the first house type.

For pigs (and ruminants), the water pool simulated in AMCLIM–Housing is determined by sources of water from urination (F_{urine}), water in faecal excreta ($F_{\text{faecal water}}$) and loss by evaporation of water (F_{evap} , mm s^{-1}). A cleaning-day function
100 is included in the equation to account for the effect of cleaning on the water pool as follows:

$$\frac{dM_{\text{H}_2\text{O}}}{dt} = F_{\text{urine}} + F_{\text{faecal water}} - F_{\text{evap}} - \psi_{\text{cleaning}}(t, \text{H}_2\text{O}) \quad (\text{S19})$$

Excess water, such as washing water or drinking water in the houses, is not included since the quantity is unknown.

The evaporation rate in the animal houses is approximated by applying an aerodynamic method using a vapor transfer coefficient (B_{vap} , $\text{m Pa}^{-1} \text{ s}^{-1}$) and vapor pressure deficit as follows (Chow et al., 1988):

$$105 \quad F_{\text{evap}} = B_{\text{vap}}(e_s - e_a), \quad (\text{S20})$$

$$B_{\text{vap}} = \frac{0.622k^2 \rho_{\text{air}} u}{\rho_{\text{water}} p \left[\ln \left(\frac{z}{z_0} \right) \right]^2}, \quad (\text{S21})$$

where e_s is the saturation vapor pressure, and e_a is the actual vapor pressure at present state. ρ_{water} is the density of water, respectively. The wind speed u (m s^{-1}) is calculated from the housing ventilation at an assumed reference height of z that equals 2 m, with roughness height z_0 is assumed to be $2 \times 10^{-3} \text{ m}$ (2 mm).

110

S3.2 Simulations for poultry housing

The third type of animal house in AMCLIM–Housing is designed specifically for poultry housing simulations. This accounts for the fact that poultry excreta are in the form of uric acid, which hydrolyses to TAN much more slowly than urea (see Sect.S2). Furthermore, poultry excreta are much drier than pig excreta, so the rate of uric acid hydrolysis is also limited by the moisture levels (Sect.S2). Housing management for poultry can also differ from other livestock. Addition of bedding materials to poultry excreta produces a solid litter. Consequently, poultry litter can be left in houses for a longer period than for other housed livestock, i.e., so called “deep litter” systems.

In AMCLIM–Housing, the water pool in poultry houses is determined by the initial water content in the excreta ($F_{\text{excretion water}}$), evaporation, and the cleaning function, as shown in the following equation:

$$120 \quad \frac{dM_{\text{H}_2\text{O}}}{dt} = \max(F_{\text{excretion water}} - F_{\text{evap}}, m_E M_{\text{DM}}) - \psi_{\text{cleaning}}(t, \text{H}_2\text{O}) \quad (\text{S22})$$

where m_E is the equilibrium moisture content of the excreta as a function of ambient temperature and humidity. M_{DM} is the mass of dry matter (DM) of the excreta, which is used to determine the water at equilibrium moisture.

The moisture in poultry litter and solid manure due to evaporation cannot decline further than a threshold and will eventually reach an equilibrium state to the ambient humidity, and evaporation is assumed to stop at this point. The litter moisture content exerts a vapor pressure on the adjacent air, and the ratio of this moisture vapor pressure to the saturated vapor pressure of pure water in air at the temperature of the material is called the equilibrium relative humidity (Henderson and Perry, 1976). If the air RH is higher than the equilibrium relative humidity of the material, the material will increase in moisture content. Conversely, the material will decrease in moisture content if the air RH is lower than the equilibrium. The equilibrium moisture content is calculated by the following equation (Elliott and Collins, 1982):

$$130 \quad m_E = \left[\frac{-\ln\left(1 - \frac{\text{RH}}{100}\right)}{0.0000534 \times T} \right]^{\frac{1}{1.41}} \quad (\text{S23})$$

The high DM content of the poultry litter can result in NH_4^+ adsorption on litter solids, a process similar to NH_4^+ adsorption on soil particles (as described in Jiang et al., submitted 2024). Due to the lack of knowledge regarding nitrogen adsorption on livestock manure, AMCLIM–Land uses a constant partitioning coefficient (K_a) of 1.0 for all livestock (Vira et al., 2020), so the amount of N adsorbed on manure solid is only dependent on the water content of the manure. Moreover, the surface of poultry excreta can dry quickly, forming a natural outer “crust” that prevents further emissions from the old litter below. The quantity of this layer is uncertain, and modelling the drying process is difficult. To simulate the NH_3 volatilization from poultry excreta, AMCLIM–Housing assumes an additional surface resistance of 8640 s m^{-1} (0.1 d m^{-1}) for litter (R_{litter}). This surface resistance is derived using an inversion method as described in the previous version of AMCLIM–Poultry (Jiang et al., 2021). For deep litter system, surface resistance is assumed to double (17280 s m^{-1} or 0.2 d m^{-1}) due to the added bedding materials used.

S3.3 Simulations for ruminant housing

Ruminants including cattle, sheep and goats, are typically kept in naturally ventilated animal houses as these animals have higher tolerances to cold temperatures than pigs and poultry. In AMCLIM, it is assumed that the excreta from these animals are removed from the houses on a daily basis. Meanwhile, ruminants also graze outside, which leads to the deposition of excreta on pastures. Two grazing systems are considered: year-round grazing and seasonal grazing. In the case of year-round grazing, all ruminant excreta are assumed to be deposited on pastures. For seasonal grazing, the excreta are split into two parts, with a fraction of excreta remaining in the animal houses, while the rest is left outside while grazing. The time evolution of N pools (M_N ; given in per unit area; all masses have units of g m^{-2} , if not otherwise specified) in the animal houses can be modified from Eq. (6) as follows:

$$150 \quad \frac{dM_{N_i}}{dt} = (1 - f_{\text{grazing}})F_{\text{excretN}}f_{N_i} - K_{N_i}M_{N_i} - \psi_{\text{cleaning}}(t, N_i), \quad (\text{S24})$$

where f_{grazing} is the fraction of ruminant excreta that is deposited on pastures and is dependent on the grazing time. As described in Sect.2.2.2, F_{excretN} is the total N excretion rate from the livestock, and f_N is the fraction of a N form in the excretion. K_N is the conversion rate (s^{-1}) at which a N species decomposes (Sect.S2). $\psi_{\text{cleaning}}(t)$ represents the cleaning event of the house (see Eq. 5).

155 The characteristics of ruminant excreta are similar to pigs, as they contain both urine and dung, with excreted N mainly existing as urea in urine and organic N in faeces. The differences between ruminant and pig excreta stem from the biological and behavioural features that are varied between livestock, such as urinary N concentration, faecal N content, urination and defecation volume/mass and frequency etc. Further information has been given in Table A1 in Appendix. The TAN pool can be calculated by Eq. (4). Similarly, the water pool is calculated from urination (F_{urine}), water in faecal excreta ($F_{\text{faecal water}}$),
160 loss by evaporation of water (F_{evap} , mm s^{-1}), and the cleaning event by the following equation:

$$160 \quad \frac{dM_{\text{H}_2\text{O}}}{dt} = (1 - f_{\text{grazing}})(F_{\text{urine}} + F_{\text{faecal water}}) - F_{\text{evap}} - \psi_{\text{cleaning}}(t, \text{H}_2\text{O}). \quad (\text{S25})$$

S4 Nitrification process of livestock manure

Nitrification is considered to take place in soils and solid manure systems exposed to oxygen. In contrast, for liquid systems, such as slurry system or lagoon, nitrification is considered to be absent or negligible due to the high water-content that reduce the oxygen availability. In the model, nitrification is included as a loss mechanism in order to calculate the TAN pool in solid phase manure management simulations.

A first-order reaction is used to determine nitrification (Parton et al., 1996a, 2001a). The optimum nitrification rate ($K_{\text{Nitrif,opt}}$) is set to be 10 % per day, and the nitrification rate K_{Nitrif} is affected by temperature, water content and pH (Parton et al., 1996, 2001). The dependence of each factor is expressed by the following equations. The temperature dependence is taken from Stange and Neue (2009):

$$k_{\text{nitrif},T} = \left(\frac{t_{\text{max}} - T_{\text{gnd}}}{t_{\text{max}} - t_{\text{opt}}} \right)^{a_{\Sigma}} \exp \left(a_{\Sigma} \left(\frac{t_{\text{max}} - T_{\text{gnd}}}{t_{\text{max}} - t_{\text{opt}}} \right) \right), \quad (\text{S26})$$

where T_{gnd} is the ground temperature. The maximum temperature (t_{max}) and optimum temperature (t_{opt}) for microbial activity is 313 K and 301 K, respectively. a_{Σ} is an empirical factor that equals to 2.4 for manure; optimum temperature is 303 K (Stange and Neue, 2009).

The water content and pH dependence are taken from the empirical function of Parton et al. (1996):

$$k_{\text{nitrif},WFPS} = \left(\frac{WFPS - b}{a - b} \right)^d \left(\frac{b - a}{a - c} \right)^d \left(\frac{WFPS - c}{a - c} \right)^d, \quad (\text{S27})$$

where $WFPS$ is the water-filled porosity of soil and is set to 1.0 for solid manure storage. Coefficients a , b , c and d equal to 0.60, 1.27, 0.0012 and 2.84, respectively (Parton et al., 1996).

$$k_{\text{nitrif},\text{pH}} = 0.56 + \frac{\tan^{-1}(0.45\pi(\text{pH}-5))}{\pi}. \quad (\text{S28})$$

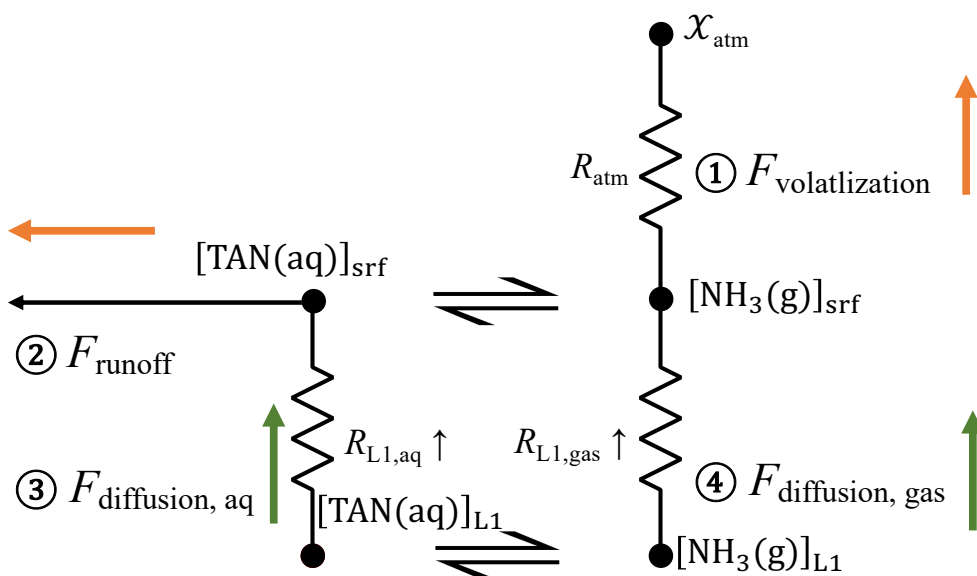
Nitrification is found to taking place in soils at pH ranging between 5.5 to 10, with the optimum pH is around 8.5 (Parton et al., 1996), and the processes ceases in soils under natural pH less than 5.0 (Parton et al., 1996). In AMCLIM-Land, the pH dependence for nitrification rate is a trigonometric function from Parton et al. (1996).

S5 Concentrations of nitrogen species at the emission surface

Volatilization take place at the emitting surface, which is primarily driven by the concentrations at the surface, in comparison with atmospheric concentration. For simulating NH_3 emissions from solid manure storage, the processes are similar to the land simulations (Jiang et al., submitted 2024). TAN is assumed to be evenly distributed in the stored manure, so the TAN concentration represents the concentration of the bulk manure ($[\text{TAN}(\text{aq})]_{\text{bulk}}$). TAN is transferred from the manure to a source layer at the surface through diffusion. The diffusion is in aqueous phase considering the water content and is constrained by manure resistance. Manure resistance is determined by dividing the thickness of the surface layer (which is assumed to be 2 cm as a surface crust) by the aqueous diffusivity of NH_4^+ . The upward diffusive fluxes are equal to the volatilization flux (as there is no runoff for housing and storage). Therefore, the TAN concentration at the manure surface can be solved by the following equation:

$$[\text{TAN}(\text{aq})]_{\text{srf}} = [\text{TAN}(\text{aq})]_{\text{bulk}} \cdot \frac{\left(\frac{1}{R_{\text{manure,aq}}} \right) + \frac{X_{\text{in}}}{R_{\text{store}}}}{\frac{1}{R_{\text{manure,aq}}} + \frac{K_{\text{NH}_3}}{R_{\text{store}}}}. \quad (\text{S29})$$

195



200 **Figure S2.** Sketch of the physical transport for nitrogen species (TAN as an example) in the top soil layer in AMCLIM-Land. Upward diffusions including aqueous and gaseous diffusive flux are equivalent to the surface runoff and volatilization to satisfy mass conservation (process 1+2 = 3+4; the sum of the fluxes represented by orange arrows = the sum of the fluxes represented green arrows).

S6 Model setup for global simulations of ammonia emission from livestock farming

S6.1 Housing environments and housing density

205 There are two housing systems considered in AMCLIM-Housing: fully enclosed houses (with forced heating and ventilation) and partially enclosed houses as described in Sect.2.2.1. The inside conditions of animal houses influence NH_3 emission from livestock housing, and they can be very different from the natural environment, with indoor temperature being the most prominent environmental factor. Pigs and poultry have a lower critical temperature (i.e., the minimum managed temperature for optimum animal performance) of approximately 16–20 °C (Gyldenkærne et al, 2005). Therefore, pigs and

210 poultry from commercial production systems that are intensively managed (e.g., industrial pigs, broilers and layers) are typically kept in insulated buildings equipped with forced heating and ventilation systems. These systems help maintain the ambient temperature within a recommended range throughout the year as far as feasible (Seedorf et al., 1998). Heating is used on cold days when the temperature is low, while ventilation is used to cool down the house when the temperature is high. Fully enclosed houses require a minimum level of ventilation to remove odours and emissions like NH_3 from the

215 house, which aims to maintain a healthy environment for the animal growth. However, the ventilation should also be below a certain rate to avoid causing an induced draft in the house.

For intermediate and backyard production systems, pigs and poultry are kept in barns that are naturally ventilated. These barns have indoor environments that are closer to the natural environments, with slightly higher temperatures than outdoor temperatures due to the warmth generated by the animals, with local materials being used to block wind and to warm the buildings on cold days.

In AMCLIM–Housing, the indoor temperature and ventilation of animal houses are modelled using a set of empirically derived relationships in relation to the outdoor temperature. These relationships are based on data from the Animal Feeding Operations (AFOs) dataset of the US Environmental Protection Agency (EPA, 2012) and theoretical parameterizations of indoor environments by Gyldenkærne et al. (2005). These relationships can vary between livestock sectors and production systems as each production system of livestock has a corresponding housing system and house type in the global simulations. Table S1 lists the housing system and house type of livestock by production systems used in AMCLIM–Housing.

Table S1. Housing systems and house types for livestock in AMCLIM–Housing.

Production system	Housing system	House type
Pigs		
Industrial	Fully enclosed house	Houses with slatted floors and storage pits
Intermediate	Naturally ventilated house	Normal barns
Backyard	Naturally ventilated house	Normal barns
Poultry		
Broiler	Fully enclosed house	Poultry houses
Layer	Fully enclosed house	Poultry houses
Backyard	Naturally ventilated house	Poultry houses
Ruminants		
Mixed	Naturally ventilated house	Normal barns

For the enclosed houses with heating and ventilation systems for pigs, the parameterizations of housing environments are taken from Gyldenkærne et al. (2005), as shown in Figure S3. The indoor temperature (T_{in} , °C) is a function of outside temperature (T_{out} , °C), as the following:

$$T_{in} = \begin{cases} T_{rec} + \Delta T_{low} \times (T_{out} - T_{min}), & \text{if } T_{out} \leq T_{min} \\ T_{rec}, & \text{if } T_{min} < T_{out} \leq T_{max} \\ T_{rec} + \Delta T_{high} \times (T_{out} - T_{max}), & \text{if } T_{max} < T_{out} \end{cases}, \quad (S30)$$

235 where T_{rec} is the recommended temperature (20 °C), ΔT_{low} is the temperature dependency (0.5 °C °C⁻¹) for temperatures below T_{min} (0 °C), ΔT_{high} is the temperature dependence (1.0 °C °C⁻¹) above T_{max} (12.5 °C).

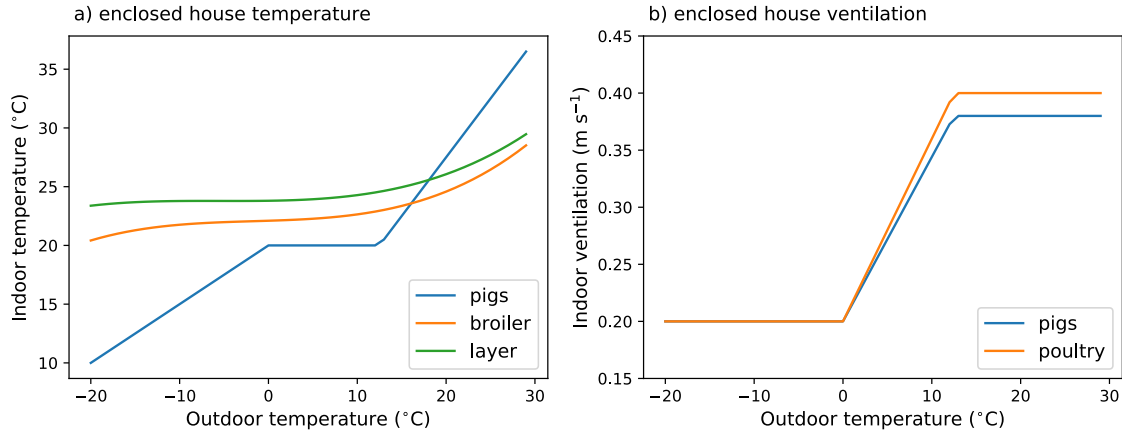
For the enclosed poultry houses, the temperature relationships are derived from the USEPA AFO dataset as the follows (as shown in Fig A3):

$$T_{in} = \begin{cases} 2.0 \times 10^{-4} T_{out}^3 + 1.0 \times 10^{-3} T_{out}^2 + 2.4 \times 10^{-2} T_{out} + 22.1, & \text{for broilers} \\ 1.4 \times 10^{-4} T_{out}^3 + 2.3 \times 10^{-3} T_{out}^2 + 1.1 \times 10^{-2} T_{out} + 23.8, & \text{for layers} \end{cases} \quad (S31)$$

240 The ventilation (V_{in} , m s⁻¹) of the enclosed animal houses calculated as follows (as shown in Fig A3):

$$V_{in} = \begin{cases} V_{min}, & \text{if } T_{out} \leq T_{min} \\ V_{min} + T_{out} \times \left(\frac{V_{max} - V_{min}}{T_{max} - T_{min}} \right), & \text{if } T_{min} < T_{out} \leq T_{max}, \\ V_{max}, & \text{if } T_{max} < T_{out} \end{cases} \quad (S32)$$

where V_{min} is the minimum ventilation (0.2 m s⁻¹), and V_{max} is the maximum ventilation rate (0.38 m s⁻¹ for pigs; 0.40 m s⁻¹ for poultry). It is worth noting that the unit of ventilation is expressed in metre per second, which should be distinguished from the ventilation rate used in Eq. (2) for conceptualising the indoor NH₃ concentration of animal houses.



245

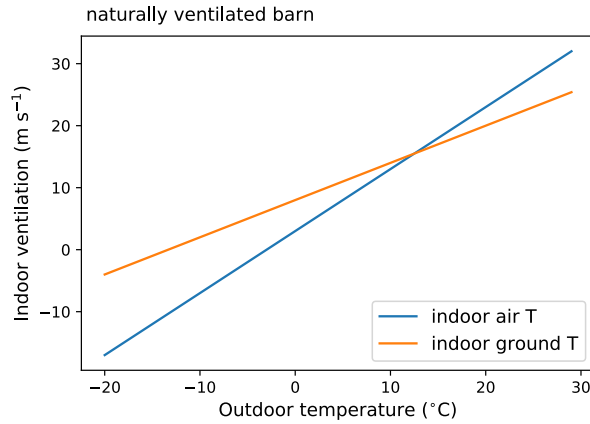
Figure S3. Modelled indoor temperature and ventilation of fully enclosed animal houses for pigs and poultry in relation to outdoor temperature.

For naturally ventilated barns where ruminants, intermediate pigs, and backyard pigs and poultry are housed, the relationship between indoor temperature and the outdoor temperature is expressed as follows as shown in Figure S4:

$$250 \quad T_{in} = T_{out} + D_{temp}, \quad (S33)$$

$$T_{floor} = T_{out} + 0.4 \times (T_{rec} - T_{out}), \quad (S34)$$

where D_{temp} is the temperature difference between indoor and outdoor temperature due to the warmth generated by animals (3 °C) and T_{floor} is floor temperature.



255 **Figure S4. Modelled indoor air and ground temperature of naturally ventilated animal barns in relation to outdoor temperature.**

The ventilation in the barns is related to the wind speed outside (u_{out} , $m s^{-1}$), which is expressed by the following equation:

$$V_{in} = (1 - f_{blocking})u_{out}, \quad (S35)$$

where $f_{blocking}$ is a blocking factor due to mechanical blocking, which is larger in cold days and smaller in warm days.

$$f_{blocking} = \begin{cases} 0.2, & \text{if } T_{out} > T_{floor} - D_{temp} \\ 0.8, & \text{if } T_{out} \leq T_{floor} - D_{temp} \end{cases} \quad (S36)$$

260 Housing density varies depending on the livestock and production system. Industrial pigs are assumed to be housed at a typical density of 120 kg liveweight per square meter (Lim et al., 2010). By comparison, intermediate and backyard pigs are housed at lower densities than the industrial production system, with assumed values of 80 and 60 kg liveweight m^{-2} , respectively. Regarding poultry housing, the assumed density for broilers and layers are 15 and 30 birds m^{-2} , respectively (Cortus et al., 2010a, b; Wang et al., 2010). Backyard poultry are less densely housed than broilers and layers, with an
 265 assumed density of 4 birds m^{-2} . For cattle, the housing density of 100 kg liveweight m^{-2} is assumed for beef, 80 kg liveweight m^{-2} for all dairy, and 150 kg liveweight m^{-2} for feedlot cattle. The housing area (S_{house} , m^2) is calculated accordingly by the following equation:

$$S_{house} = \begin{cases} \frac{n_i m_i}{den_{housing}}, & \text{if } i \text{ is pig} \\ \frac{n_i}{den_{housing}}, & \text{if } i \text{ is poultry} \end{cases}, \quad (S37)$$

where n_i and m_i are the number of animals and average body weight ($kg head^{-1}$), and $den_{housing}$ is the housing density of the
 270 livestock ($kg animal m^{-2}$ for pigs and number of animal m^{-2} for chicken). It is worth noting that pig houses with slatted floor and pit have two NH_3 -emitting surfaces, so the slats areas (S_{slats} , m^2) and pit areas (S_{pit} , m^2) are calculated separately:

$$\begin{cases} S_{slats} = (1 - f_{gap})S_{housing} \\ S_{pit} = f_{pit}S_{housing} \end{cases}, \quad (S38)$$

where f_{gap} is the fraction of gap space in the slats (assumed to be 0.2, i.e., gap represents 20 % of floor area, for global simulation), and f_{pit} is the relative area of the pit to the housing area (set to be 1.0 in AMCLIM–Housing, meaning that the pit surface has an equivalent size as the area of the house).

To estimate housing NH_3 emissions in global simulations, it is assumed that indoor and atmospheric NH_3 concentrations are negligible, given that animal houses are significant NH_3 sources and their surface concentrations are much higher than indoor and outdoor concentrations. However, as the global volume of animal houses is uncertain (as described in Equation 4.2), the calculation of NH_3 emissions is simplified by using the following equation:

$$F_{\text{NH}_3} = \frac{\chi_{\text{srf}}}{R_{\text{G,house}}}. \quad (\text{S39})$$

S6.2 Manure storage and manure application

Ammonia emissions from livestock housing, manure storage and land application of manure are closely interrelated. In particular, there are several management systems related to housing that should be specifically pointed out as relevant for calculation of NH_3 emissions. In houses with slatted floor and pits, manure can be stored in the house pit either for long-term or short-term periods. For long-term pit storage, excreta are assumed in AMCLIM to be stored for two months (60 days) before being applied to the land. For short-term storage, excreta are removed from the pit daily and stored in a separate storage unit (also for the naturally ventilated barns) before ultimately being applied to the land. The specific in-situ storage management systems are determined by the MMS information in the GLEAM database.

For broiler housing with litter management, AMCLIM assumes that excretions remain in the houses for the entire year, being applied to land once being removed. It should be noted that the NH_3 emissions from in-situ storage are counted as part of housing emissions. In contrast, naturally ventilated barns are assumed to be cleaned daily so that excreta are removed from the house and are stored separately.

Livestock excreta removed from the houses are typically stored for a certain period before being applied to the land. However, the area of the storage facilities is uncertain. In the AMCLIM model, it is assumed that the area for manure storage (S_{storage}) is proportional to the housing area, which is expressed as:

$$S_{\text{storage}} = f_{\text{MMS}} f_{\text{store-housing}} S_{\text{housing}}, \quad (\text{S40})$$

where f_{MMS} is the fraction of manure that is removed for separate storage as part of the MMS. The ratio of storage area to housing area ($f_{\text{store-housing}}$) varies depending on the specific management system. The ratio is set to be 0.5 for liquid manure storage and 0.25 for solid manure storage, and 2.5 for lagoon management, given that liquid manure storage requires a larger area because the volumes are larger than those of solid manure.

In AMCLIM, it is assumed that the stored manure is kept for 180 days and then is applied to the land twice a year during the spring and autumn planting seasons, respectively. The application date is based on the average value of the crop calendars for 18 spring crops and 4 winter crops. For slurry application, the application rate is assumed to be 3 mm of slurry,

305 which is equivalent to a recommended rate of 30 tons per hectare. For solid manure application, a moderate fertilization rate of 10 tons per hectare is used. The N pools and the water pool are calculated accordingly. It should be noted that all stored manure, with the exception of manure in lagoons, is assumed to be applied to agricultural lands. The lagoon system is a small fraction (< 1 % of total managed manure N) among all management systems, and manure in this system is assumed not to be applied to land, but to be kept in the lagoons in AMCLIM.

310 **S6.3 Grazing density**

The grazing density for all cattle is set at 2500 m² per head (equivalent to 4 animals ha⁻¹; Saarijärvi et al., 2006; Saarijärvi and Virkajärvi, 2009). For sheep and goats, a housing density of 50 kg liveweight m⁻² is assumed and a grazing density of 400 m² per head (equivalent to 25 animals ha⁻¹). The housing areas are calculated by Eq. (S37) as for pigs. For grazing, the area (S_{grazing} , m²) can be calculated by the following equation:

$$315 \quad S_{\text{grazing}} = n_i \text{den}_{\text{grazing}} \quad (\text{S41})$$

Note that grazing “density” ($\text{den}_{\text{grazing}}$, m² head⁻¹) has a different unit from housing density ($\text{den}_{\text{housing}}$, kg animal weight m⁻²) as mentioned. It is important to clarify that the source areas of NH₃ emissions from grazing are not equivalent to the grazing area. Saarijärvi et al. (2006) have shown that the annual average surface coverage of urine and dung on a grazing field is 17 % and 4 %, respectively. In AMCLIM, the source areas of NH₃ emissions from urine patch ($S_{\text{urine patch}}$) and dung pat ($S_{\text{dung pat}}$)

320 can be expressed as follows:

$$S_{\text{urine patch}} = f_{\text{urine}} S_{\text{grazing}}, \quad (\text{S42})$$

$$S_{\text{dung}} = f_{\text{dung}} S_{\text{grazing}}, \quad (\text{S43})$$

where f_{urine} is 0.17 and f_{dung} is 0.04. The areas for dung-only and dung mixtures in the dung pat scheme are the same, which accounts for 2 % of the total grazing area.

325 **S7 Site simulations of layer-chicken housing using AMCLIM**

Figure S5 shows the simulated NH₃ emissions and indoor concentrations of a layer house compared with the measurements, along with indoor conditions and modelled N species. The indoor environments of the layer house are similar to the pig houses (Fig. 4 and Fig. A1-A3), with temperature being largely maintained between 20 to 30 °C throughout the year and ventilation working intensively in hot summer. Relative humidity inside the layer house shows strong daily variations, 330 ranging between 40 to 80 %.

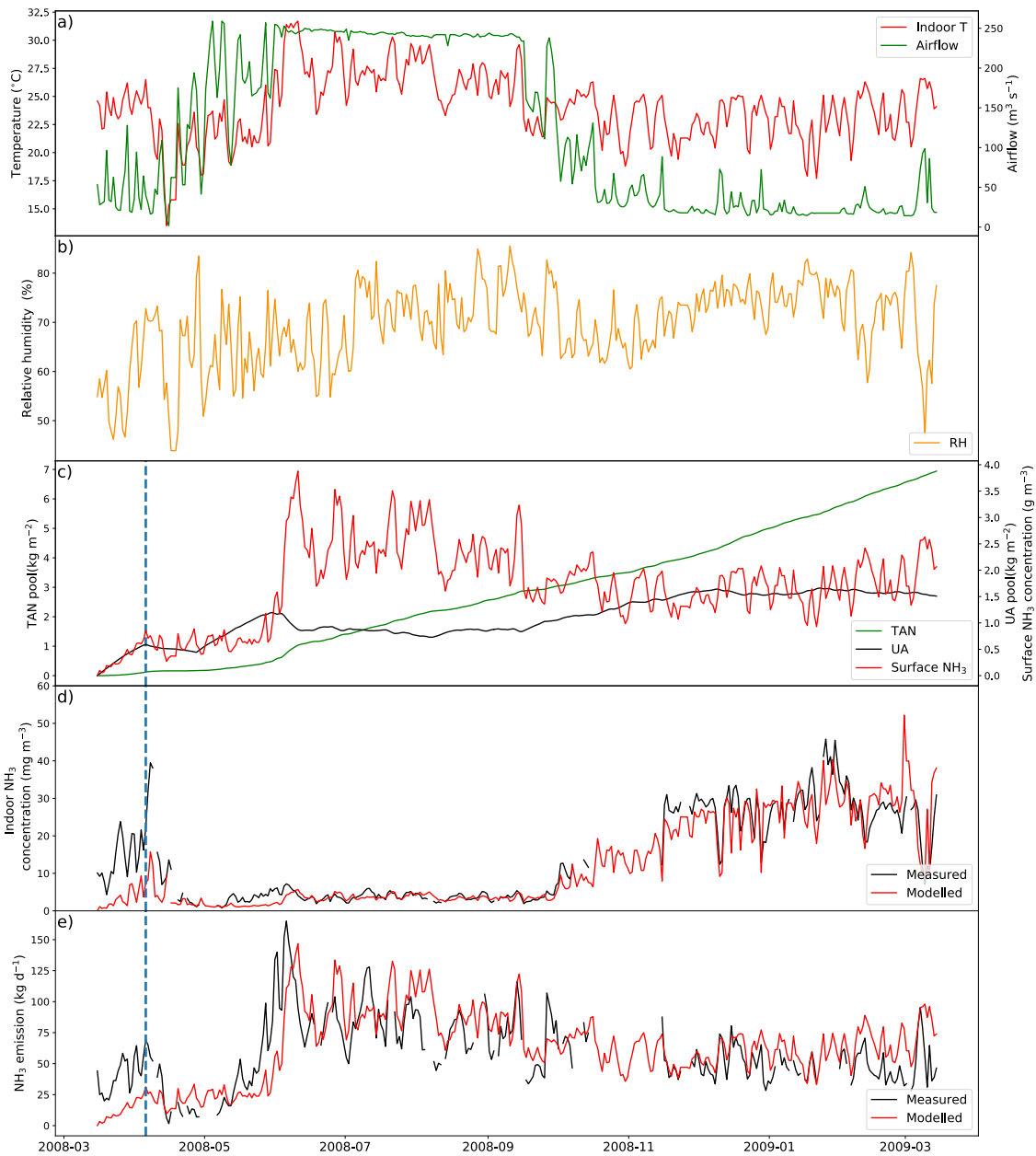
The simulated period is from 15 March 2008 to 15 March 2009. The house was fully occupied by more than 90 000 layers for most of the time and was only emptied once (on 04 April 2008) for three weeks. Overall, the model captures the major changes of NH₃ emissions and indoor concentrations well over the simulation period. High emissions occur in summer as the ventilation increases, with the emissions peaking in early June 2008. The maximum daily NH₃ emission is more than 150 kg 335 d⁻¹, and AMCLIM–Housing roughly reproduces this value but with a lag of ~5 days, in the timing of the peak in early June

2008. The average daily emission of NH_3 estimated by the model is 63.6 kg d^{-1} (when measurements available; 62.4 kg d^{-1} for the entire simulation), compared to 54.4 kg d^{-1} reported by the measurements. Approximately 34 % of total excreted N is lost due to NH_3 emissions according to the simulation.

340 The indoor NH_3 concentrations show an opposite trend to the emission, which is inversely related to the ventilation. The indoor NH_3 level is typically lower than 10 mg m^{-3} when the airflow rate is high in summer and was much higher in the winter when the ventilation decreases, reaching to around 30 mg m^{-3} from November 2008 to February 2009. AMCLIM–Housing replicates the measured indoor NH_3 concentration well. However, the model largely underestimates both the emissions and concentrations in the first simulated month before the house is emptied. The measured NH_3 concentration at the surface is much higher than the simulated indoor concentrations, ranging from 0.5 to 4.0 g m^{-3} (500 to 4000 mg m^{-3}),
345 which generates a concentration gradient that drives the emission fluxes. As this concerns the start of the simulation period, this may reflect uncertainties in the influence of previous housing conditions.

As shown Figure S5, the uric acid pool in the excreta gradually increases in the first three months of the simulation and then generally stabilizes in the remaining period. There are two decreases in the simulated uric acid pool, with the first drop due to the emptying of the house in early April 2008 and the second due to a sharp increase of indoor temperature that
350 accelerates the hydrolysis process in late May 2008. By comparison, the TAN pool accumulates throughout the year, building up to about 7 g N m^{-2} at the end of the simulation. It is notable that the variations in surface concentration of NH_3 are similar to those in NH_3 emissions. This is because the litter resistance (8640 s m^{-1}) is much larger than the housing resistance that range between 200 to 600 s m^{-1} . As a result, the total resistances show small variability. The NH_3 emissions are mainly constrained by the litter resistance, so the emissions and concentrations broadly display the same feature.

355 Compared with Jiang et al. (2021), the major updates of current model version have been summarised and discussed in Sect.2.6 and Sect.4.5. For site simulations of chicken housing, relevant changes include incorporation of TAN adsorption on manure particles, more realistic water balance, inclusion of organic forms of N from excreta and a new resistance scheme which is dependent on environmental factors. These modifications lead to a better representation of the processes than the previous Poultry Model which uses calibrated resistances, without compromising model performance.



360

Figure S5. Site simulations of House A in a layer-chicken farm at site NC2B, Nash, North Carolina, from 15 March 2008 to 15 March 2009. (a) Measured daily mean indoor temperature and airflow rate of the house. (b) Measured daily mean relative humidity of the house. (c) Modelled Total Ammoniacal Nitrogen (TAN) pool and Uric Acid (UA) pool. (d) Comparison between measured and modelled indoor NH₃ concentrations of the house and surface NH₃ concentrations. (e) Comparison between modelled NH₃ emissions and calculated NH₃ emissions from measured indoor concentrations. Vertical blue dashed lines refer to emptying of the house. The simulations applied the site air-flow (m³ s⁻¹) as reported by reference.

365

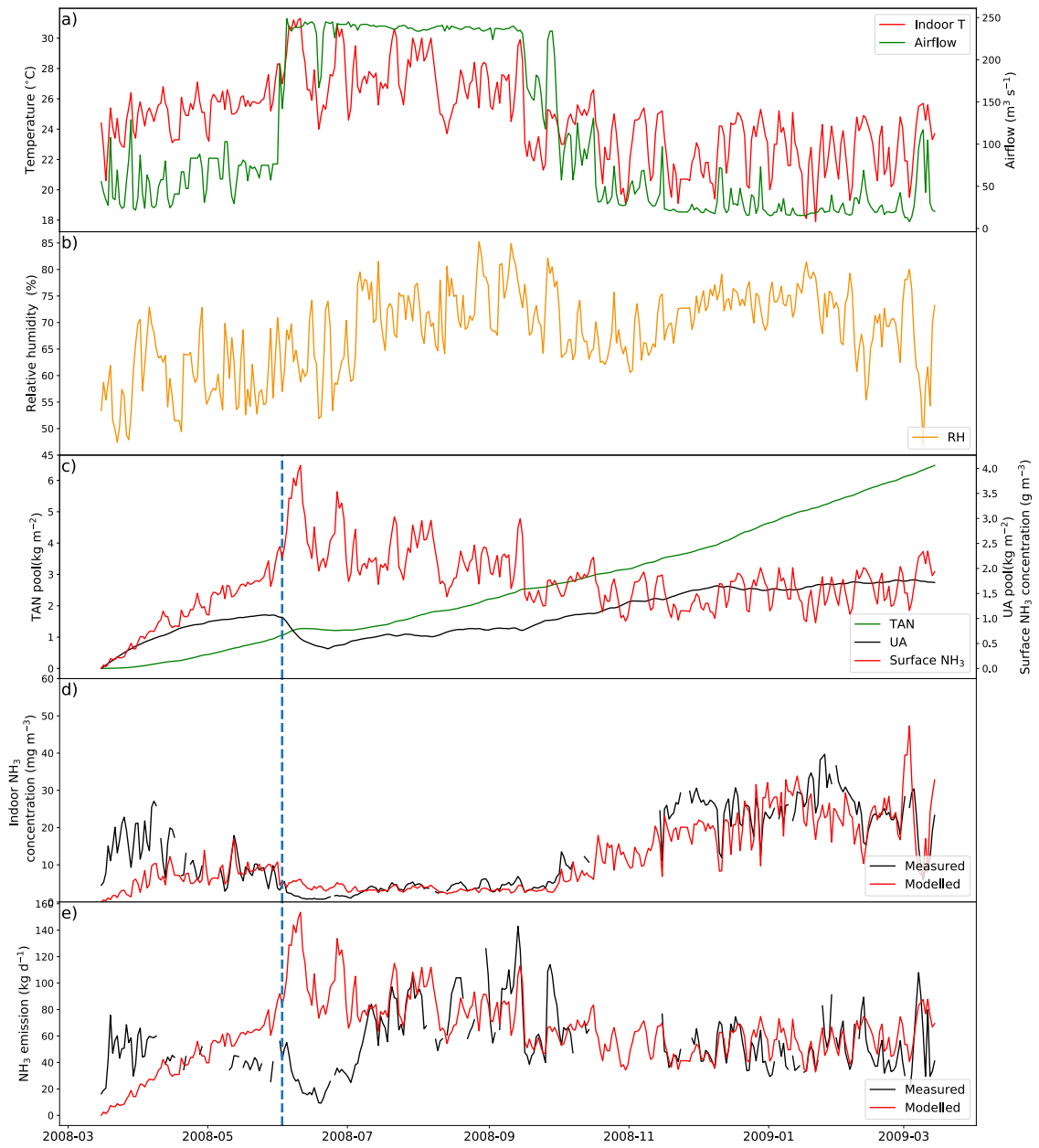


Figure S6. Same as Figure S5, but for House B at site NC2B.

References

- Chow, V. T., Maidment, D. R., and Mays, L. W.: Applied hydrology, [Nachdr.], internat. ed. 1988., McGraw-Hill, New York, 572 pp., 1988.
- 375 Cortus, E. L., Lin, X.-J., Zhang, R., and Heber, A. J.: National Air Emissions Monitoring Study: Emissions Data from Two Broiler Chicken Houses in California - Site CA1B. Final Report, Purdue University, 2010a.
- Cortus, E. L., Lin, X.-J., Zhang, R., and Heber, A. J.: National Air Emissions Monitoring Study: Emissions Data from Two Layer Houses in California - Site CA2B. Final Report, Purdue University, 2010b.
- Elliott, H. A. and Collins, N. E.: Factors Affecting Ammonia Release in Broiler Houses, Transactions of the ASAE, 25, 380 0413–0418, <https://doi.org/10.13031/2013.33545>, 1982.
- Gilmour, J. T., Cogger, C. G., Jacobs, L. W., Evanylo, G. K., and Sullivan, D. M.: Decomposition and Plant-Available Nitrogen in Biosolids, Journal of Environment Quality, 32, 1498, <https://doi.org/10.2134/jeq2003.1498>, 2003.
- Gyldenkærne, S.: A dynamical ammonia emission parameterization for use in air pollution models, J. Geophys. Res., 110, D07108, <https://doi.org/10.1029/2004JD005459>, 2005.
- 385 Haynes, R. J. and Williams, P. H.: NUTRIENCYCLINAGND SOILFERTILITY IN THE GRAZEPDASTUREECOSYSTEM, Advances in Agronomy, 1993.
- Henderson, S. M. and Perry, R. L.: Agricultural process engineering, 3d ed., Avi Pub. Co, Westport, Conn, 442 pp., 1976.
- Jiang, J., Stevenson, D. S., Uwizeye, A., Tempio, G., and Sutton, M. A.: A climate-dependent global model of ammonia emissions from chicken farming, Biogeosciences, 18, 135–158, <https://doi.org/10.5194/bg-18-135-2021>, 2021.
- 390 Lim, T. T., Chen, L., Jin, Y., Ha, C., Ni, J.-Q., Bogan, B. W., Ramirez, J. C., Diehl, C., Xiao, C., and Heber, A. J.: National Air Emissions Monitoring Study: Emissions Data from Four Swine Finishing Rooms - Site IN3B. Final Report, Purdue University, 2010.
- Liss, P. S. and Slater, P. G.: Flux of Gases across the Air-Sea Interface, Nature, 247, 181–184, <https://doi.org/10.1038/247181a0>, 1974.
- 395 Ni, J.: Mechanistic Models of Ammonia Release from Liquid Manure: a Review, Journal of Agricultural Engineering Research, 72, 1–17, <https://doi.org/10.1006/jaer.1998.0342>, 1999.
- Parton, W. J., Mosier, A. R., Ojima, D. S., Valentine, D. W., Schimel, D. S., Weier, K., and Kulmala, A. E.: Generalized model for N₂ and N₂O production from nitrification and denitrification, Global Biogeochem. Cycles, 10, 401–412, <https://doi.org/10.1029/96GB01455>, 1996.
- 400 Parton, W. J., Holland, E. A., Del Grosso, S. J., Hartman, M. D., Martin, R. E., Mosier, A. R., Ojima, D. S., and Schimel, D. S.: Generalized model for NO_x and N₂O emissions from soils, J. Geophys. Res., 106, 17403–17419, <https://doi.org/10.1029/2001JD900101>, 2001.
- Riddick, S., Ward, D., Hess, P., Mahowald, N., Massad, R., and Holland, E.: Estimate of changes in agricultural terrestrial nitrogen pathways and ammonia emissions from 1850 to present in the Community Earth System Model, Biogeosciences, 405 13, 3397–3426, <https://doi.org/10.5194/bg-13-3397-2016>, 2016.

Saarijärvi, K. and Virkajärvi, P.: Nitrogen dynamics of cattle dung and urine patches on intensively managed boreal pasture, *J. Agric. Sci.*, 147, 479–491, <https://doi.org/10.1017/S0021859609008727>, 2009.

410 Saarijärvi, K., Mattila, P. K., and Virkajärvi, P.: Ammonia volatilization from artificial dung and urine patches measured by the equilibrium concentration technique (JTI method), *Atmospheric Environment*, 40, 5137–5145, <https://doi.org/10.1016/j.atmosenv.2006.03.052>, 2006.

Seedorf, J., Hartung, J., Schröder, M., Linkert, K. H., Pedersen, S., Takai, H., Johnsen, J. O., Metz, J. H. M., Groot Koerkamp, P. W. G., Uenk, G. H., Phillips, V. R., Holden, M. R., Sneath, R. W., Short, J. L. L., White, R. P., and Wathes, C. M.: A Survey of Ventilation Rates in Livestock Buildings in Northern Europe, *Journal of Agricultural Engineering Research*, 70, 39–47, <https://doi.org/10.1006/jaer.1997.0274>, 1998.

415 Sherlock, R. and Goh, K.: Dynamics of ammonia volatilization from simulated urine patches and aqueous urea applied to pasture I. Field experiments, *Fertilizer Research*, 5, 181–195, <https://doi.org/10.1007/BF01052715>, 1984.

Sherlock, R. and Goh, K.: Dynamics of ammonia volatilization from simulated urine patches and aqueous urea applied to pasture. II. Theoretical derivation of a simplified model, *Fertilizer Research*, 6, 3–22, <https://doi.org/10.1007/BF01058161>, 1985.

420 Sommer, S. G. and Hutchings, N. J.: Ammonia emission from field applied manure and its reduction—invited paper, *European Journal of Agronomy*, 15, 1–15, [https://doi.org/10.1016/S1161-0301\(01\)00112-5](https://doi.org/10.1016/S1161-0301(01)00112-5), 2001.

Stange, C. F. and Neue, H.-U.: Measuring and modelling seasonal variation of gross nitrification rates in response to long-term fertilisation, *Biogeosciences*, 6, 2181–2192, <https://doi.org/10.5194/bg-6-2181-2009>, 2009.

425 Vigil, M. F. and Kissel, D. E.: Rate of Nitrogen Mineralized from Incorporated Crop Residues as Influenced by Temperature, *Soil Science Society of America Journal*, 59, 1636–1644, <https://doi.org/10.2136/sssaj1995.03615995005900060019x>, 1995.

Wang, K., Kilic, K. I., Li, Q., Wang, L., Bogan, W. L., Ni, J.-Q., Chai, L., and Heber, A. J.: National Air Emissions Monitoring Study: Emissions Data from Two Tunnel-Ventilated Layer Houses in North Carolina - Site NC2B. Final Report, Purdue University, 2010.

430